nature communications

Matters arising

https://doi.org/10.1038/s41467-025-66247-0

DFT calculations and theory do not support enantiospecificity in NMR J-coupling constants

Received: 29 April 2025

Accepted: 3 November 2025

Published online: 14 November 2025

Check for updates

Frédéric A. Perras[1,2] ✉, Josef W. Zwanziger[3] & Aaron J. Rossini[1,2]

ARISING FROM T. Georgiou et al. *Nature Communications* https://doi.org/10.1038/s41467-024-49966-8 (2024)

Distinguishing the enantiomers of small organic molecules is an industrially relevant problem with important implications for the health of the population[1]. In a recent publication, Bouchard and co-workers have suggested that large differences in indirect spin-spin (*J*) coupling constants between enantiomers are possible[2]. A close inspection of their work revealed significant flaws in their density functional theory (DFT) calculations and that the reported effects disappear with appropriate care. We thus conclude that enantiospecificity in spin-spin coupling constants has not be demonstrated either experimentally or theoretically.

The most common approach used to measure the population of enantiomers is chromatography using a chiral medium. Nuclear magnetic resonance (NMR) spectroscopy has long been known to be insensitive to enantiomers, because enantiomers yield identical NMR spectra. The resonance frequencies in these spectra are determined by the chemical shift and *J* coupling interactions of the various nuclear spins in the sample, which are forcibly identical for the two enantiomers. To separate the NMR signals from two enantiomers in a racemic mixture it is necessary to render them diastereomeric either using a chiral medium[3], via the reaction with a second enantiopure molecule[4], or by the application of an oscillating electric field[5].

To the best of our knowledge, it has never been observed that the solution NMR spectrum of a racemic mixture yields two sets of resonances for the two enantiomers within an ordinary NMR apparatus. This observation is consistent with Ramsey's theory for magnetic shielding[6], and its extension to *J* coupling[7], which depends on factors which are invariant with respect to mirror symmetry operations.

We were thus extremely surprised when the aforementioned communication reported DFT calculated predicted differences in ^{1}H-^{1}H, ^{1}H-^{13}C, and ^{13}C-^{13}C *J* coupling constants between enantiomers that differed by more than 10 Hz[2]. In solution-phase NMR spectra *J* couplings are typically reported to a precision of 0.1 Hz, thus such differences in J coupling constants for enantiomers should be experimentally observable in racemic mixtures of enantiomeric compounds. We believe that there are simpler explanations as to why their DFT calculations predicted different coupling constants for enantiomers.

The first issue is that the molecular geometries used for DFT calculations on the D and L molecules (and provided in their Supplementary data) had significant structural differences. The coordinates used for calculations did not have mirror symmetry, thus, the calculations were not performed on true enantiomers. Shown in Fig. 1 are overlays of the geometries used for the L and D isomers for the twelve compounds studied. The coordinates of the D enantiomer were subjected to a reflection operation and the structures were overlaid using the Chem3D program. Figure 1 clearly shows that there are significant differences in the conformation of the backbone carbons, the orientation of the NH_2 and COOH moieties, and in one case (alanine) an extra fluoride ion was added to the D enantiomer. Only three structures could be said to approximate mirror symmetry (glutamic acid, phenylalanine, and tyrosine).

However, even for glutamic acid, phenylalanine, and tyrosine, significant differences in computed *J* coupling values were reported for stereoisomers. Investigation of the values reported in the supplementary material, revealed there are likely significant issues with the calculations themselves. Namely, one-bond ^{13}C-^{13}C *J* coupling constants, which typically are of approximately 40 Hz, are reported to be around 170 Hz. We thus repeated the DFT calculations of the *J* coupling constants in D and L-alanine (the compound discussed in the main text) at the PBE0/TZ2P level of theory[8] using the Amsterdam Density Functional (ADF) software[9] and its highest density integration grid[10] (known colloquially as 'excellent') (see Table 1). Spin-orbit coupling was also added using the zeroth-order regular approximation (ZORA)[11,12], given that it was implied in the theory. Our calculations yielded *J* coupling constants that are closer in line with experiment. Most importantly, we also did not observe any difference between the computed values for the two enantiomers (Fig. 2).

Shown in Fig. 2 are bar graphs of the normalized difference in *J* coupling constants between the D and L enantiomers of alanine from the prior publication and this work. As can be seen, we can obtain small differences in *J* coupling constants of a few percent when performing independent geometry optimizations of the two enantiomers. These mHz differences in predicted *J* coupling constants likely arise due to

[1]Ames National Laboratory, Ames, IA, USA. [2]Department of Chemistry, Iowa State University, Ames, IA, USA. [3]Department of Chemistry, Dalhousie University, Halifax, NS, Canada. ✉e-mail: fperras@ameslab.gov

https://doi.org/10.1038/s41467-025-66247-0

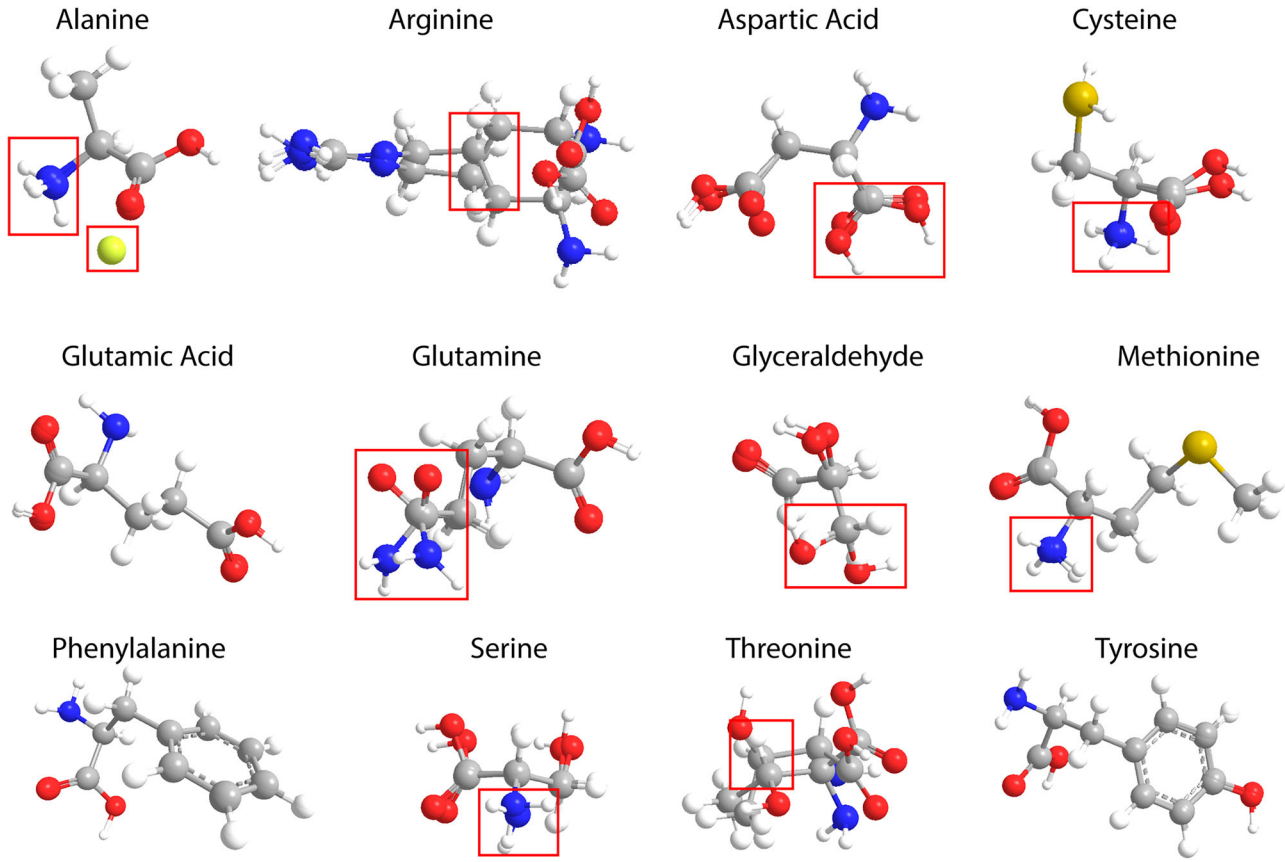

Fig. 1 | Overlays of the structures for twelve of the D (inverted coordinates) and L molecules that were used for DFT calculations reported by Bouchard and co-workers (ref. 2). None of the structures are related by mirror symmetry and thus they are not truly enantiomers. Nine of the twelve structures further have quite significant structural differences, as outlined in the red boxes. Specifically, models differ in **a** the addition of extra atoms (alanine), **b** backbone conformations (arginine, glutamine, glyceraldehyde, threonine), **c** orientation of the NH_2 (alanine, cysteine, methionine, serine), or the orientation of the carboxyl (aspartic acid).

the finiteness of the integration grid and the convergence criteria, but none of the differences are as large as those that were reported. If both structures are made to be true enantiomers of one another by applying a mirror symmetry operation to the molecular coordinates, then the difference in calculated J coupling constants vanishes.

As such, when DFT calculations are performed with larger basis sets, finer integration grids, and using mirror-symmetric isomers, the conclusions from the Bouchard and co-workers report are not reproduced. Software programs, such as ORCA[13] and ADF[9] do not predict differing J coupling constants for enantiomers with fully converged calculations. Note that such errors are unlikely to occur in achiral molecules owing to the use of identical internal coordinates by the software.

From a theoretical perspective, the internuclear spin-spin elements (D_{ij}^{kl}) computed above between nuclear dipoles k and l, which contains both through-space (dipolar) and through-bond (J) contributions, arise from the following energy derivative:

$$D_{ij}^{kl} = \frac{1}{2}\frac{\partial^2 E}{\partial \mu_i^k \partial \mu_j^l} \tag{1}$$

In Eq. 1, E is the total energy of the system while μ_i^k denotes component I of the dipole moment on atom k.

The Hohenberg-Kohn theorems show that the total energy E may be written exactly as

$$E[\rho] = T[\rho] + V_{ee}[\rho] + V_{ext}[\rho] \tag{2}$$

where each term is a functional of the electron density. The terms are the kinetic energy T, the electron-electron energy V_{ee}, and the external potential V_{ext}, which here represents the interactions of the electrons with the atomic nuclei. Notice that this energy expression is exact, despite the fact that it is not known how to compute it exactly. In any case, the only term in it that depends on the atomic positions is the external potential, which can be represented in atomic units as follows, assuming N atoms and M electrons

$$V_{ext} = \sum_{k=1}^{N}\sum_{m=1}^{M}\frac{-Z_k}{\left|\vec{r}_m - \vec{R}_k\right|} \tag{3}$$

In this form, electron m is at position $\vec{r}_m$, and nucleus k carries charge Z_k and is located at $\vec{R}_k$. Notice that the nuclear dipole energies are not included here; that is because they are so small that they do not renormalize the electron interactions (in other words, their effect is so weak compared to the electrostatic interactions that they may be added perturbatively).

For any isolated molecule, the Hamiltonian, or here, the external potential, is invariant under the operations of the point group of the molecule. For a pair of enantiomers, mirror symmetry is not one of these operations. Instead, each enantiomer under reflection is transformed into the partner molecule, which is distinguishable from it, but crucially, all internuclear distances (and therefore also angles) in the external potential are unchanged. Therefore, the electron density of the transformed molecule will be identical to that of the original, except mirrored, and all bond distances and angles will be identical. Therefore, the total energy will be unchanged.

https://doi.org/10.1038/s41467-025-66247-0

Table 1 | Comparison of the DFT-calculated ^{13}C-^{1}H and ^{13}C-^{13}C *J* coupling constants for D- and L-alanine from this work and the prior publication

		J coupling constant (Hz)			
nuc 1	nuc 2	D-Ala (this contribution)	L-Ala (this contribution)	D-Ala (pub.)	L-Ala (pub.)
C_β	C_α	36.528	36.528	127.25	111.56
C_β	H_{COO}	−0.544	−0.544	−0.45	−0.44
C_β	$H_{NH2,1}$	4.843	4.843	11.3	3.25
C_β	$H_{NH2,2}$	−0.89	−0.89	1.39	−0.62
C_β	C_{COO}	−2.463	−2.463	−9.22	−9.94
C_β	$H_{\beta,1}$	147.32	147.32	172.88	175.73
C_β	$H_{\beta,2}$	153.319	153.319	178.4	177.06
C_β	$H_{\beta,3}$	148.723	148.723	180.78	175.44
C_β	H_α	−3.769	−3.769	−8.51	−5.86
C_α	H_{COO}	9.727	9.727	7.23	8.21
C_α	$H_{NH2,1}$	−2.759	−2.759	−5.26	−3.85
C_α	$H_{NH2,2}$	−5.341	−5.341	−5.96	−5.42
C_α	C_{COO}	68.1	68.1	166.61	179.38
C_α	$H_{\beta,1}$	−5.174	−5.174	−6.83	−6.3
C_α	$H_{\beta,2}$	−4.876	−4.876	−3.6	−6.31
C_α	$H_{\beta,3}$	−2.221	−2.221	−6.62	−3.61
C_α	H_α	168.462	168.463	169.27	175.18
C_{COO}	$H_{\beta,1}$	3.029	3.029	2.3	2.26
C_{COO}	$H_{\beta,2}$	10.969	10.969	0.59	9.85
C_{COO}	$H_{\beta,3}$	1.663	1.663	9.89	0.9
C_{COO}	Hα	−8.466	−8.466	−6.96	−8.84
H_{COO}	$H_{NH2,1}$	1.471	1.471	−0.08	0
H_{COO}	$H_{NH2,2}$	−0.076	−0.076	−0.21	−0.1
H_{COO}	C_{COO}	−7.813	−7.813	−7.61	−7.56
H_{COO}	$H_{\beta,1}$	0.07	0.07	0.14	0.05
H_{COO}	$H_{\beta,2}$	−0.072	−0.072	−0.02	−0.06
H_{COO}	$H_{\beta,3}$	0.037	0.037	−0.15	−0.09
H_{COO}	H_α	0.682	0.682	−0.31	0.54
$H_{NH2,1}$	$H_{NH2,2}$	−11.495	−11.495	−11.71	−9.69
$H_{NH2,1}$	C_{COO}	12.414	12.414	1.12	11.27
$H_{NH2,1}$	$H_{\beta,1}$	−0.409	−0.409	−0.2	−0.34
$H_{NH2,1}$	$H_{\beta,2}$	−0.535	−0.535	3.67	−0.35
$H_{NH2,1}$	$H_{\beta,3}$	−0.65	−0.65	0.02	−0.45
$H_{NH2,1}$	H_α	−0.246	−0.246	2.43	0.08
$H_{NH2,2}$	C_{COO}	6.031	6.031	1.56	3.9
$H_{NH2,2}$	$H_{\beta,1}$	−0.206	−0.206	−0.04	−0.16
$H_{NH2,2}$	$H_{\beta,2}$	−0.229	−0.229	−0.4	−0.25
$H_{NH2,2}$	$H_{\beta,3}$	−0.621	−0.621	−0.27	−0.67
$H_{NH2,2}$	H_α	13.721	13.721	15.63	13.42
$H_{\beta,1}$	$H_{\beta,2}$	−13.407	−13.408	−13.9	−13.23
$H_{\beta,1}$	$H_{\beta,3}$	−13.621	−13.621	−13.69	−13.42
$H_{\beta,1}$	H_α	14.749	14.749	13.68	13.11
$H_{\beta,2}$	$H_{\beta,3}$	−15.054	−15.054	−13.56	−14.38
$H_{\beta,2}$	H_α	6.232	6.232	3.24	5.41
$H_{\beta,3}$	H_α	2.156	2.156	5.4	2.22

Furthermore, the terms D_{ij}^{kl} will also be unchanged (albeit transposed[14,15], so that the eigenvalues of the D_{ij}^{kl} matrix are invariant), because they depend precisely on the locations the nuclear dipole moments, which are located at the nuclear sites. Because all bond distances and angles are unchanged, the couplings are as well. Put more mathematically, the couplings as derivatives depend only on local data at each nuclear site, which is identical between the two partners. This conclusion is identical for both "through bond" and "through space" coupling mechanisms. Additionally, the fact that nuclear dipoles are pseudovectors and thus carry information on orientation, unlike regular vectors, is not a concern here because the couplings are bilinear in the dipole moments. Hence, the couplings always depend on a pair of moments and possible additional sign changes under reflections are always cancelled.

To attempt to develop a mechanism that could potentially show a difference between enantiomers, we can argue along the lines of recent work on the natural optical activity tensor, which is essentially the spatial dispersion of the dielectric function[16,17]. In that case, a third order response must be computed, of the following form:

$$E^{(3)} = \frac{\partial^3 E}{\partial q_m \partial E_i \partial E_j} \tag{4}$$

in which the wavevector $\vec{q}$ describes the spatial dependence, and the E_i, E_j are components of the electric field of the light that generates the dielectric response function. In the present case, we would like to find the spatial dispersion of the nuclear dipole coupling **D**, and so one is led to consider

$$E^{(3)} = \frac{\partial^3 E}{\partial q_m \partial \mu_i^k \partial \mu_j^l} \tag{4}$$

The necessary density functional perturbation theory for such expressions has been fully developed[18], and implemented for a variety of responses, including optical activity[16]. Due to the "2n + 1" theorem[18], in all these cases the necessary third-order energy may be obtained from knowledge of the zeroth and first order wavefunctions only. In the optical activity case, the first order wavefunctions arise from perturbing the zeroth order wavefunctions and charge density by the electric field, which is a strong perturbation. In the nuclear dipole case, however, the first order perturbation is due to the nuclear dipole interaction. First order perturbation theory provides the simple estimate that the wavefunction perturbation has size $||H^1||/\Delta E$, where ΔE is the energy gap to the excited states. For the nuclear dipole interaction, $||H^1|| \sim J \sim 10^2$ Hz, while the gap is typically at least 1 eV (2.418×10^{14} Hz), if not more. This estimate then gives a ratio of 10^{-13} or less, so such a third order mechanism, at least of this type, is surely too weak to show any difference between enantiomers.

We lastly think that it is necessary to comment on the calculations of ^{1}H-^{1}H *J* couplings in a DNA molecule[2]. These calculations make the following assertions that disagree with experiment and theory on many fronts:

1. In Fig. 2a of ref.[2], they calculate ^{1}H-^{1}H spin-dipole *J* coupling constants of the order of 100,000 Hz (as explicitly stated in the caption to Fig. 2 in the original publication) for spin pairs separated by a very large number of bonds. $^{3}J_{HH}$ couplings are known to be roughly in the range from -5 to +15 Hz.
2. They suggest that *J* coupling constants should differ in spin pairs related by rotational symmetry. Specifically, that *J* coupling values at coordinates (φ_1, φ_2) and $(\varphi_1 + \theta, \varphi_2 + \theta)$ should be different. This arises from the use of wavefunction that describes DNA as a conductor.
3. They do not calculate the isotropic average of the spin-dipole contribution, which is anisotropic, unlike Fermi contact, and instead only calculate a single tensor element (the 'zz' component), which would of course depend on the orientation of the spin pair.
4. They suggest that *J* coupling constants are invariant of the internuclear distance, as seen by the calculation of large *J* coupling constants when $\Delta\varphi$ is large (Fig. 2a–d in the original publication).

https://doi.org/10.1038/s41467-025-66247-0

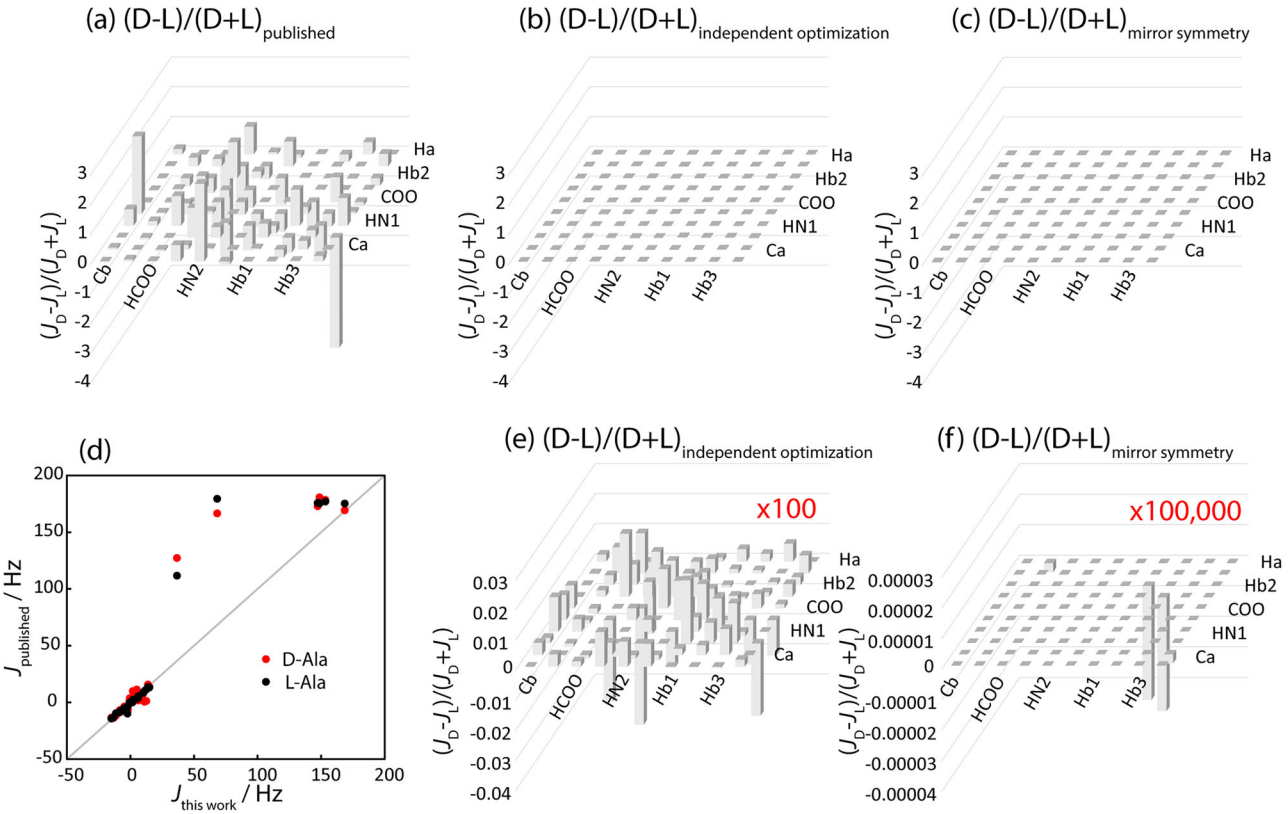

Fig. 2 | Relative differences between calculated *J* coupling constants in D- and L-alanine. a Data taken from ref. 2. Calculated values in (**b**) and (**e**) were obtained from the independent optimizations of the two enantiomers and highlight minor geometrical differences that arise due to the integration grid and finite convergence criteria while those in (**c**) and (**f**) are exactly mirror symmetric. In (**c**) and (**f**) some *J* coupling values for the enantiomers deviate by up to 30 μHz, likely due to the finite integration grid. In (**d**) are plotted the correlations between the calculated *J* coupling constants from this work and ref. 2. This plot highlights non-physical deviations for certain calculated *J* coupling constants.

5. They calculate that the Fermi contact term, which depends on *s*-orbital overlap, is largest when $\Delta\varphi$ is largest, namely, when the two nuclei are separated by the greatest distance (Fig. 2c, d in the original publication).
6. They predict that the spin-dipole mechanism should dominate for ^{1}H and ^{13}C, which goes against well-known periodic trends in *J* coupling mechanisms[19]. For ^{1}H and ^{13}C, Fermi contact contributions to *J* couplings are most significant.

Most importantly, however, they did not demonstrate that the *J* coupling constant would change for the opposite helicity and so these calculations do not show enantiospecificity.

To conclude, we believe there are several significant issues with the recent work of Bouchard and co-workers. Their DFT calculations were performed on pairs of chiral molecules that were not truly enantiomers because they had different conformations. In one case, calculations were even performed on molecules with different formulas. Here we demonstrated that performing calculations with high-quality integration grids on true enantiomers of alanine results in identical *J* coupling constants, consistent with prior literature precedent. Consideration of the theory underlying the DFT calculation of such *J* couplings indicate that they are not in fact enantiospecific and have no significant dispersive response.

Methods

All density functional theory (DFT) calculations were performed using the Amsterdam Density Functional (ADF) software (ver. 2021.104)[9] using the highest density integration grid[10] (known colloquially as 'excellent'). Calculations used the hybrid functional PBE0[8] with the TZ2P basis set. Spin-orbit relativistic effects were included using the zeroth-order regular approximation (ZORA)[11,12]. The structures for D- and L-alanine were optimized independently, their coordinates are as Supplementary Data. A single-point *J* coupling calculation was further done on a D-alanine model created by the inversion of the x coordinates form the optimized L-alanine geometry to have perfect mirror symmetry. Differences between the two structures originate from the convergence criteria and the finite integration grid. The calculated *J* coupling constants are given in Table 1 whereas the full calculation input and output files are given as Supplementary Data.

Data availability

The full calculation input and output files for the calculations reported in this publication are provided as Supplementary data.

References

1. Smith, S. W. Chiral toxicology: it's the same thing...only different. *Toxicol. Sci.* **110**, 4–30 (2009).
2. Georgiou, T. et al. Enantiospecificity in NMR enabled by chirality-induced spin selectivity. *Nat. Commun.* **15**, 7367 (2024).
3. Lafontaine, E., Bayle, J. P. & Courtieu, J. High-resolution NMR in cholesteric medium: visualization of enantiomers. *J. Am. Chem. Soc.* **111**, 8294–8296 (1989).
4. Vashistha, V. K. Chiral analysis of pharmaceuticals using NMR spectroscopy: a review. *Asian J. Org. Chem.* **11**, e202200544 (2022).
5. Buckingham, A. D. & Fischer, P. Direct chiral discrimination in NMR spectroscopy. *Chem. Phys.* **324**, 111–116 (2006).
6. Ramsey, N. F. Magnetic shielding of nuclei in molecules. *Phys. Rev.* **78**, 699–703 (1950).

7. Ramsey, N. F. Electron coupled interactions between nuclear spins in molecules. *Phys. Rev.* **91**, 303–307 (1953).
8. Perdew, J. P., Ernzerhoff, M. & Burke, K. Rationale for mixing exact exchange with density functional approximations. *J. Chem. Phys.* **105**, 9982–9985 (1996).
9. te Velde, G. et al. Chemistry with ADF. *J. Comput. Chem.* **22**, 931–967 (2001).
10. Franchini, M., Philipsen, P. H. T. & Visscher, L. The Becke fuzzy cells integration scheme in the amsterdam density functional program suite. *J. Comput. Chem.* **34**, 1819–1827 (2013).
11. van Lenthe, E., Baerends, E. J. & Snijders, J. G. Relativistic regular two-component Hamiltonians. *J. Chem. Phys.* **99**, 4597–4610 (1993).
12. Autschbach, J. & Ziegler, T. Nuclear spin–spin coupling constants from regular approximate relativistic density functional calculations. II. Spin–orbit coupling effects and anisotropies. *J. Chem. Phys.* **113**, 9410–9418 (2000).
13. Neese, F. Software update: The ORCA program system—Version 5.0. *WIREs Comput. Mol. Sci.* **12**, e1606 (2022).
14. King, J. P., Sjolander, T. F. & Blanchard, J. W. Antisymmetric couplings enable direct observation of chirality in nuclear magnetic resonance spectroscopy. *J. Phys. Chem. Lett.* **8**, 710–714 (2017).
15. Garbacz, P. & Vaara, J. Direct enantiomeric discrimination through antisymmetric hyperfine coupling. *Chem. Commun.* **57**, 8264–8267 (2021).
16. Zabalo, A. & Stengel, M. Natural optical activity from density-functional perturbation theory. *Phys. Rev. Lett.* **131**, 086902 (2023).
17. Royo, M. & Stengel, M. First-principles theory of spatial dispersion: dynamical quadrupoles and flexoelectricity. *Phys. Rev. X* **9**, 021050 (2019).
18. Gonze, X. Adiabatic density-functional perturbation theory. *Phys. Rev. A* **52**, 1096–1114 (1995).
19. Bryce, D. L. & Wasylishen, R. E. Indirect nuclear spin–spin coupling tensors in diatomic molecules: a comparison of results obtained by experiment and first principles calculations. *J. Am. Chem. Soc.* **122**, 3197–3205 (2000).

Acknowledgements

We would like to thank Profs. David L. Bryce and Lyndon Emsley for their valuable input on a draft of the manuscript. This work was supported by the U.S. Department of Energy (DOE), Office of Basic Energy Sciences, Division of Chemical Sciences, Geosciences, and Biosciences through a DOE Early Career Project (FAP). Ames National Laboratory is operated for the DOE by Iowa State University under Contract No. DE-AC02-07CH11358.

Author contributions

All DFT calculations were performed by F.A.P. Theoretical descriptions were derived by J.W.Z. Analysis and composition of the manuscript were performed by F.A.P., A.J.R., and J.W.Z.

Competing interests

The authors declare no competing interests.

Additional information

Supplementary information The online version contains supplementary material available at https://doi.org/10.1038/s41467-025-66247-0.

Correspondence and requests for materials should be addressed to Frédéric A. Perras.

Peer review information *Nature Communications* thanks Gustavo Aucar, Stanislav Komorovsky, and the other anonymous reviewer(s) for their contribution to the peer review of this work.